Available online at www.sciencedirect.com
SCIENCE DIRECT®
Journal of Sound and Vibration 266 (2003) 394–404
JOURNAL OF SOUND AND VIBRATION
www.elsevier.com/locate/jsvi

Letter to the Editor

Dynamic analysis of a planar rigid-link mechanism with rotating slider joint and clearance

Eleonor D. Stoenescu, Dan B. Marghitu*

Mechanical Engineering Department, Auburn University, 202 Ross Hall, Auburn, AL 36849-5341, USA

Received 11 March 2002; accepted 17 December 2002

1. Introduction

One of the important factors that influence the dynamic stability and the performance of mechanisms is the joint clearance. In the last years, many researchers have studied the effects of the clearance on the motion of mechanical systems. Farahanchi and Shaw [1] considered the model of a planar, rigid-link mechanism with clearance at the slider joint. They observed that the response of the system appears to be chaotic, although periodic motion become more common as dissipation effects are increased. Abarbanel [2–4] developed dynamic tools for analyzing observed chaotic data. Non-linear dynamic tools were presented by Nayfeh and Balachadran [5]. Deck and Dubowski [6] studied the problems encountered in predicting the dynamic response of machines with clearance connections. Recent research has contributed to the development of simulation methods for specific multibody systems. Gilmore and Cipra [7] discussed a simulation method for planar dynamical mechanical systems with changing topologies. The information provided by the rigid bodies' boundary descriptions was used to automatically predict and detect impacts. Conti et al. [8] described a unified method to predict the contact changes due to kinematics. Contact and friction constraints were used by Pfeiffer [9] to study the stick–slip phenomena. Brach [10] considered only single collisions and formulates the impact equations using Newton's law. Jean and Moreau [11] reformulated Newton's law in an unilateral manner for multiple impacts with friction. In this work, the models of rigid-body impacts described by Marghitu [12,13] were used.

In the present paper, the dynamic behavior of a planar, rigid-link mechanism with a sliding joint clearance is investigated. Periodic motion is observed for the system with no clearance. The response of the system with clearance is chaotic at relatively high crank speeds and low values of the coefficient of restitution.

*Corresponding author. Tel.: +1-334-844-3335; fax: +1-334-844-3307.
E-mail address: marghitu@eng.auburn.edu (D.B. Marghitu).

0022-460X/03/$ - see front matter
doi:10.1016/S0022-460X(03)00053-1

2. Mathematical model

In this section, the model of the mechanism is described and the equations of motion are derived. The basic assumptions are provided first. Next, differential equations which govern the dynamics of the system are presented.

2.1. Basic assumptions

In order to study the effects of clearances on the motion of a connecting rod in a slider crank mechanism, a simplified model is used, shown in Fig. 1. The following basic assumptions are considered: (1) All components are rigid. (2) All motions occur in a fixed plane. (3) A motor with a variable torque is used to crank the mechanism. (4) The clearances for the slider are symmetrically placed about the nominal slider path, that is, without clearance, and have a fixed magnitude. (5) The impacts between the connecting rod and slider are instantaneous and are modelled using a constant coefficient of restitution, a coefficient of friction, and a moment coefficient.

2.2. Equations of motion

Several methods are used to derive the equations of motion for the mechanism. It is assumed that during the impacts the system position does not change, because the impact time is very small. It is also assumed that the effect of finite forces is neglected during the impact. Formulation of rigid-body collision problems are based on two physical laws, Coulomb's law of dry friction and balance of momentum. To solve the impact equations, additional relations are obtained using a coefficient of restitution and a coefficient of friction.

Fig. 1 shows a planar slider joint where the backlash has been made very large in order to make it clearly visible. Fig. 2 illustrates a possible geometry for the slider joint with clearance and four possible cases consisting of the following: Case (a): no contact (Fig. 2(a)). Case (b): contact or impact on a single point (Fig. 2(b)). Case (c): contact or impact on two opposed points (Fig. 2(c)). Case (d): contact or impact on two points on the same side (Fig. 2(d)).

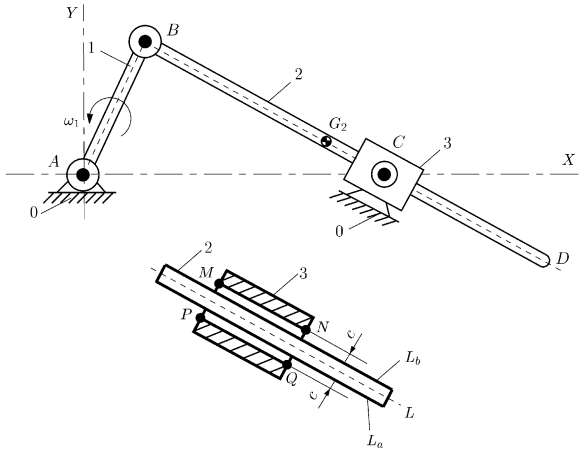

Fig. 1. Simplified model of the rigid-link mechanism with rotating slider joint and clearance.

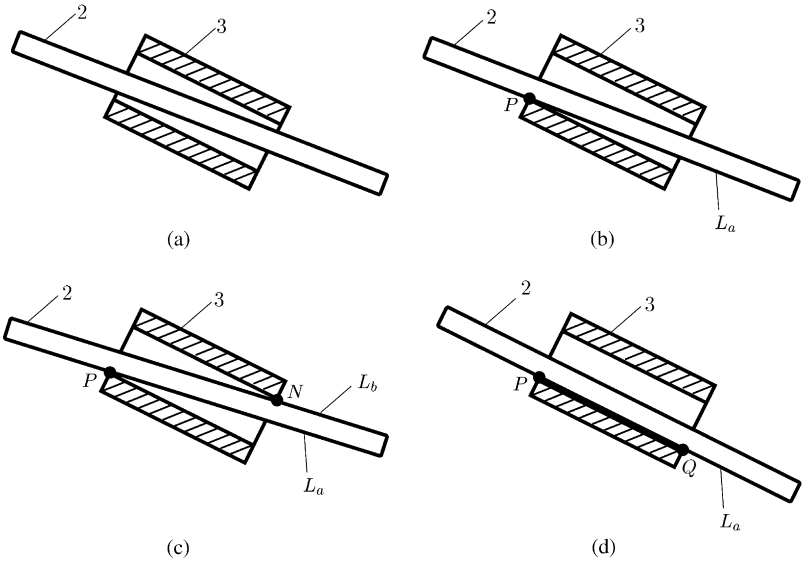

Fig. 2. Geometry of the slider joint with clearance for (a) no contact, (b) contact or impact on a single point, (c) contact or impact on two points on the same side, (d) contact or impact on two opposed points.

The conditions for switching from one case to a different one depend on the positions of the links and the reaction forces at the contact points.

Impacts can occur when the joint is in either case (b), (c) or (d). The impact conditions depend on the relative linear velocities of the contact points. For example, in case (b), one can write the following impact condition:

$$\mathbf{v}_{P_2}^n - \mathbf{v}_{P_3}^n \approx 0, \tag{1}$$

where $\mathbf{v}_{P_2}^n$ and $\mathbf{v}_{P_3}^n$ are the normal velocities to the collision surface of the contact point P between links 2 and 3.

The contact conditions also depend on the reaction forces between the links at the contact points. For example, in case (b), the force condition can be written as

$$\mathbf{N}_{P_2}^n - \mathbf{N}_{P_3}^n \approx 0, \tag{2}$$

where $\mathbf{N}_{P_2}^n$ and $\mathbf{N}_{P_3}^n$ are the reaction forces between links 2 and 3 at the contact point P.

The motion of the contact point during the impact can be described by one of the following two cases:

1. The contact point is slipping along surface while interacting with it in the normal direction. Since contact is maintained and slipping occurs, the normal and tangential components of the contact forces can be represented for dry friction as $F_t = -\mu_k F_n$.
2. The contact point is not slipping along but interacting with it in the normal direction. The tangential velocity v_t of the contact point is $v_t = 0$ subject to $|F_t/F_n| \leqslant \mu_s$.

The simulation algorithm for the mechanism automatically determines when a change in the topology occurs and reformulate the equations of motion to reflect the changes in the system

topology. The equations of motion depend on the contact and impact conditions. Sets of non-linear equations are solved for contact and sets of linear equations are solved for impact.

Next, the equations of motion for cases (a) and (b) are derived.

2.2.1. No contact

In this section, the mechanism with two degrees of freedom is considered (Fig. 3(a)). One can choose the generalized co-ordinates $q_1 = \theta_1$ and $q_2 = \theta_2$. The equation of motion is derived using Lagrange's equations

$$\frac{\mathrm{d}}{\mathrm{d}t}\left(\frac{\partial T}{\partial \dot{q}_i}\right) - \frac{\partial T}{\partial q_i} = Q_i, \quad i = 1, 2, \tag{3}$$

where T is the kinetic energy, q_i is the generalized co-ordinate, and Q_i is the generalized force associated with the co-ordinate q_i.

The kinetic energy T_1 for link 1 is

$$T_1 = \tfrac{1}{2} m_1 \mathbf{v}_{G_1} \cdot \mathbf{v}_{G_1} + \tfrac{1}{2} I_{G_1} \boldsymbol{\omega}_1 \cdot \boldsymbol{\omega}_1, \tag{4}$$

where $\boldsymbol{\omega}_1 = \dot{q}_1 \mathbf{k}$.

The kinetic energy T_2 for link 2 is

$$T_2 = \tfrac{1}{2} m_2 \mathbf{v}_{G_2} \cdot \mathbf{v}_{G_2} + \tfrac{1}{2} I_{G_2} \boldsymbol{\omega}_2 \cdot \boldsymbol{\omega}_2, \tag{5}$$

where $\boldsymbol{\omega}_2 = \dot{q}_2 \mathbf{k}$.

The total kinetic energy T is

$$T = T_1 + T_2. \tag{6}$$

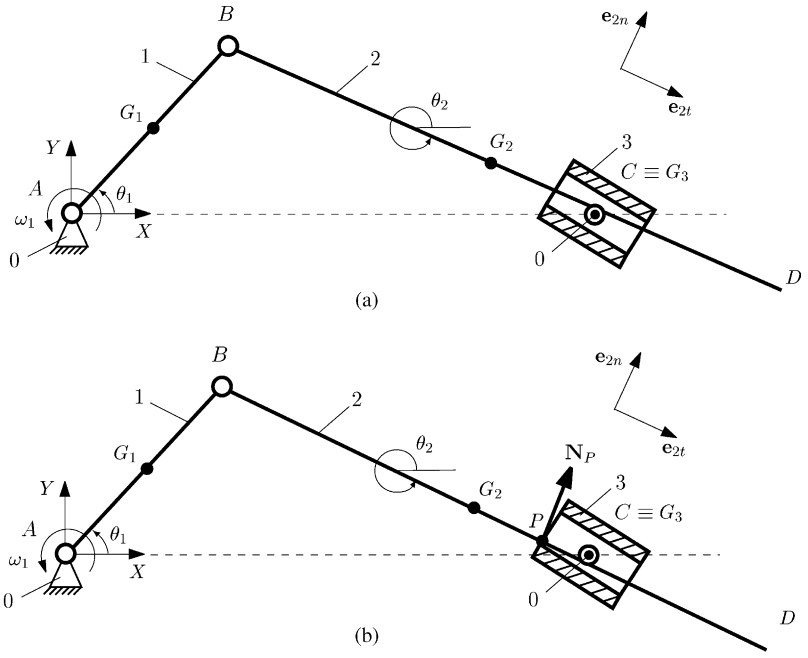

Fig. 3. Geometry of the mechanism for (a) no contact, (b) contact or impact on a single point.

One can write the generalized force Q_1 as

$$Q_1 = -(\tfrac{1}{2}m_1 + m_2)L_1 g \cos q_1. \tag{7}$$

One can write the generalized force Q_2 as

$$Q_2 = -\tfrac{1}{2}m_2 L_2 g \cos q_2. \tag{8}$$

From Eqs. (3), (6), and (7), one can write

$$\left(\frac{m_1 L_1^2}{4} + m_2 L_1^2 + I_{G_2}\right)\ddot{q}_1 + \tfrac{1}{2}m_2 L_1 L_2[\ddot{q}_2 \cos(q_2 - q_1) - \dot{q}_2^2 \sin(q_2 - q_1)] = -L_1\left(\tfrac{1}{2}m_1 + m_2\right)g \cos q_1. \tag{9}$$

From Eqs. (3), (6), and (8), one can write

$$\left(\frac{m_2 L_2^2}{4} + I_{G_2}\right)\ddot{q}_2 + \tfrac{1}{2}m_2 L_1 L_2\left[\ddot{q}_1 \cos(q_2 - q_1) + \dot{q}_1^2 \sin(q_2 - q_1)\right] = -\tfrac{1}{2}L_2 m_2 g \cos q_2. \tag{10}$$

Eqs. (9) and (10) are used and the equation of motion is solved.

2.2.2. Contact on a single point

In this case, the mechanism has two degrees of freedom (Fig. 3(b)). One can choose the generalized co-ordinates $q1 = \theta_1$ and $q_2 = \theta_2$. Kane's equations are used and the equation of motion is derived.

The total kinetic energy T is

$$T = T_1 + T_2 + T_3. \tag{11}$$

One can find the position vector $\mathbf{r}_P$ of the contact point $P(x_P, y_P)$ solving the system of equations

$$\tan q_2 = \frac{y_B - y_P}{x_B - x_P}, \quad (x_C - x_P)^2 + (y_C - y_P)^2 = r^2. \tag{12}$$

The angular velocity and acceleration vectors $\boldsymbol{\omega}_3$ and $\boldsymbol{\alpha}_3$ of link 3 are

$$\boldsymbol{\omega}_3 = \dot{\theta}_3 \mathbf{k}, \quad \boldsymbol{\alpha}_3 = \ddot{\theta}_3 \mathbf{k}, \tag{13}$$

where $\theta_3 = \arctan y_P/(x_P - AC)$.

One can choose the generalized speeds u_1 and u_2

$$u_1 = \dot{q}_1, \quad u_2 = \dot{q}_2. \tag{14}$$

In order to take in consideration the reaction force N_P between links 2 and 3 acting at the point P one can introduce a new generalized speed u_3 in the expression of the relative velocity $\mathbf{v}_{P_{23}}$:

$$\mathbf{v}_{P_{23}} = \mathbf{v}_{P_2} - \mathbf{v}_{P_3} + u_3 \mathbf{e}_{2n}, \tag{15}$$

where $\mathbf{v}_{P_2} = \mathbf{v}_{G_2} + \boldsymbol{\omega}_2 \times (\mathbf{r}_P - \mathbf{r}_{G_2})$ and $\mathbf{v}_{P_3} = \boldsymbol{\omega}_3 \times (\mathbf{r}_P - \mathbf{r}_C)$.

The reaction force $\mathbf{N}_P$ of link 3 on link 2 is

$$\mathbf{N}_P = N_P \mathbf{e}_{2n}. \tag{16}$$

The friction force $\mathbf{F}_{f_P}$ that acts on link 2 at the point P is

$$\mathbf{F}_{f_P} = -\frac{\mathbf{v}_P}{|\mathbf{v}_P|}\mu_k N. \tag{17}$$

The generalized forces Q_j, for $j = 1, 2, 3$, can be computed as

$$Q_j = \sum_{i=1}^{3} \frac{\partial \mathbf{v}_{G_i}}{\partial u_j} \cdot \mathbf{G}_i + \frac{\partial \mathbf{v}_{P_2}}{\partial u_j} \cdot (\mathbf{N}_P + \mathbf{F}_{f_P}) + \frac{\partial \mathbf{v}_{P_3}}{\partial u_j} \cdot (-\mathbf{N}_P - \mathbf{F}_{f_P}) + \frac{\partial \boldsymbol{\omega}_1}{\partial u_j} \cdot \mathbf{M}_m. \tag{18}$$

The generalized inertia forces F_j^*, for $j = 1, 2, 3$, can be written as

$$F_j^* = \sum_{i=1}^{3} \frac{\partial \mathbf{v}_{G_i}}{\partial u_j} \cdot (-m_i \mathbf{a}_{G_i}) + \sum_{i=1}^{3} \frac{\partial \boldsymbol{\omega}_i}{\partial u_j} \cdot (-I_{G_i} \boldsymbol{\alpha}_i). \tag{19}$$

One can write three Kane equations associated with the generalized speeds u_j, for $j = 1, 2, 3$:

$$F_j^* + Q_j = 0. \tag{20}$$

From Eqs. (14) and (20) one can find the equation of motion for the mechanism and the reaction force N.

2.2.3. Impact on a single point

Next, the mechanism with three generalized co-ordinates is considered (Fig. 3(b)). One can choose $q_3 = \theta_3$ as the third generalized co-ordinate.

To derive the equation of motion for the impact, an integrated form of Lagrange's equations is used:

$$\left(\frac{\partial T}{\partial \dot{q}_i}\right)_{t_s} - \left(\frac{\partial T}{\partial \dot{q}_i}\right)_{t_a} = P_i, \quad i = 1, 2, 3, \tag{21}$$

where T is the kinetic energy, $\dot{q}_i$ is the velocity associated with the generalized co-ordinate q_i, P_i is the generalized impulse associated with the co-ordinate q_i, and t_a, t_s are the times of approach and separation for the impact.

The kinetic energy T_3 for link 3 is

$$T_3 = \tfrac{1}{2} I_{G_3} \boldsymbol{\omega}_3 \cdot \boldsymbol{\omega}_3 = \tfrac{1}{2} I_{G_3} \dot{q}_3^2, \tag{22}$$

where $\boldsymbol{\omega}_3 = \dot{q}_3 \mathbf{k}$.

The total kinetic energy T is

$$T = T_1 + T_2 + T_3. \tag{23}$$

One can write the left-hand sides of Eq. (21) as

$$\left(\frac{\partial T}{\partial \dot{q}_i}\right)_{t_s} - \left(\frac{\partial T}{\partial \dot{q}_i}\right)_{t_a} = \left.\frac{\partial T}{\partial \dot{q}_i}\right/_{\dot{q}_i = \Omega_i - \omega_i}, \quad i = 1, 2, 3, \tag{24}$$

where $\omega_i = \omega_i(t_a) = \dot{q}_i(t_a)$ and $\Omega_i = \omega_i(t_s) = \dot{q}_i(t_s)$ are the angular velocities associated with the co-ordinates q_i before and after the impact.

One can express the position vector $\mathbf{r}_P$ of the impact point $P(x_P, y_P)$ solving the system of equations:

$$\tan q_2 = \frac{y_B - y_P}{x_B - x_P}, \quad \tan q_3 = \frac{y_C - y_P}{x_C - x_P}. \tag{25}$$

The velocity vector of the impact point P is $\mathbf{v}_P = \dot{\mathbf{r}}_P$.

The generalized impulses (right-hand sides of Eq. (21)) can be written as

$$P_i = \frac{\partial \mathbf{v}_P}{\partial \dot{q}_i} \cdot (F_n \mathbf{e}_{2n} + F_t \mathbf{e}_{2t}), \quad i = 1, 2, 3, \tag{26}$$

where $\mathbf{e}_{2n} = -\sin q_2 \mathbf{\imath} + \cos q_2 \mathbf{J}$ and $\mathbf{e}_{2t} = \cos q_2 \mathbf{\imath} + \sin q_2 \mathbf{J}$ are the unit vectors normal and tangential to the contact surface, and F_n, F_t are the normal and the tangential components of the impulse momentum F.

For link 1, one can write

$$\left(\frac{m_1 L_1^2}{4} + m_2 L_1^2 + I_{G_1}\right)(\Omega_1 - \omega_1) + \tfrac{1}{2} m_2 L_1 L_2 (\Omega_2 - \omega_2) \cos(q_2 - q_1) = P_1. \tag{27}$$

For link 2 one can write

$$\left(\frac{m_2 L_2^2}{4} + I_{G_2}\right)(\Omega_2 - \omega_2) + \tfrac{1}{2} m_2 L_1 L_2 (\Omega_1 - \omega_1) \cos(q_2 - q_1) = P_2. \tag{28}$$

For link 3 one can write

$$I_{G_3}(\Omega_3 - \omega_3) = P_3. \tag{29}$$

The velocities $\mathbf{v}_{P_2}$ and $\mathbf{v}_{P_3}$ of the contact points P_2 and P_3 located on links 2 and 3 can be expressed as

$$\mathbf{v}_{P_2} = \mathbf{v}_B + \dot{q}_2 \mathbf{k} \times \mathbf{BP}, \quad \mathbf{v}_{P_3} = \dot{q}_3 \mathbf{k} \times \mathbf{CP}, \tag{30}$$

where $\mathbf{v}_B = \dot{\mathbf{r}}_B$ is the linear velocity of the joint B, and $\mathbf{CP} = \mathbf{r}_P - AC\mathbf{\imath}$.

One can write the velocity of approach $\mathbf{v}_a$ and separation $\mathbf{v}_s$ for the impact as

$$\mathbf{v}_a = \mathbf{v}_{P_2}(t_a) - \mathbf{v}_{P_3}(t_a), \quad \mathbf{v}_s = \mathbf{v}_{P_2}(t_s) - \mathbf{v}_{P_3}(t_s). \tag{31}$$

From the definition of the coefficient of restitution e, one can write

$$e = -\frac{v_{sn}}{v_{an}}, \tag{32}$$

where $v_{an} = \mathbf{v}_a \cdot \mathbf{e}_{2n}$ and $v_{sn} = \mathbf{v}_s \cdot \mathbf{e}_{2n}$ are the projections of the linear velocities of approach and separation $\mathbf{v}_a$ and $\mathbf{v}_s$ on the normal direction $\mathbf{e}_{2n}$.

The tangential component $\mathbf{v}_{st}$ of the velocity of separation vector $\mathbf{v}_s$ can be expressed as

$$\mathbf{v}_{st} = (\mathbf{v}_s \cdot \mathbf{e}_{2t}) \mathbf{e}_{2t}. \tag{33}$$

There are two cases of impact with friction at the point P:

(1) *No slipping*: The following condition must be satisfied:

$$\left|\frac{F_t}{F_n}\right| < \mu_s. \tag{34}$$

In this case, the velocity vector $\mathbf{v}_{st}$ is zero:

$$\mathbf{v}_{st} = \mathbf{0}. \tag{35}$$

From Eqs. (27)–(29), (32), and (35) one can find the unknown variables F_n, F_t, and Ω_i, $i = 1, 2, 3$.

(2) *Slipping*: The following condition must be satisfied:

$$\left|\frac{F_t}{F_n}\right| > \mu_s. \tag{36}$$

In this case, the following relation can be written as

$$F_t \mathbf{e}_{2n} = -\frac{\mathbf{v}_{st}}{|\mathbf{v}_{st}|}\mu_k |F_n|. \tag{37}$$

From Eqs. (27)–(29), (32), and (37), one can find the unknown variables F_n, F_t, and Ω_i, $i = 1, 2, 3$.

For cases (c) and (d) one can use similar assumptions and derive the equations of motion using the same methods.

3. Lyapunov exponents

Data obtained from a deterministic system can be classified as either periodic or non-periodic [5]. Non-periodic data may correspond to a quasiperiodic, transient or chaotic motion. The term chaotic is assigned to those problems for which there are no random or unpredictable variable or parameters, but their time histories have a sensitive dependence on initial conditions. Thus, the motion is chaotic in the sense of not being predictable when there is a small uncertainty in the initial conditions. The chaotic motion is characterized by a continuous, broadband Fourier spectrum and is possible only in a three-or-more dimensional non-linear system of differential equations.

The Lyapunov exponents provide a measure of the sensitivity of the system to its initial conditions. They exhibit the average rate at which nearby trajectories converge or diverge in the state space and are used to distinguish the chaotic and non-chaotic behaviors. Periodic systems show only negative and zero exponents which indicate the convergence to a predictable motion. A positive exponent means that two close trajectories that start from almost identical conditions will move apart at an exponential rate as the time evolves. This rate, and hence the predictability of the system, is described by the largest of the Lyapunov exponents. Therefore, one needs to determine the sign of the Lyapunov exponents in order to characterize the behavior of the dynamic system.

4. Numerical results

In this section, results from computer simulations are presented using analysis tools. In Fig. 1 the mechanism with slider clearance is shown. The masses of the links are $m_1 = 0.008$ kg, $m_2 = 0.038$ kg, and $m_3 = 0.015$ kg. The mass moments of inertia for the links are $I_{G_1} = 6.733 \times 10^{-6}$ kg m^3, $I_{G_2} = 6.925 \times 10^{-4}$ kg m^3, and $I_{G_3} = 2.220 \times 10^{-6}$ kg m^3. The lengths of links are

$L_1 = 0.1$ m, $L_2 = 0.47$ m, and $L_3 = 0.047$ m. The nominal width of the slider (link 3) is $l_3 = 0.025$ m. The distance between the pin joints A and C is $AC = 0.28$ m. The kinetic coefficient of friction $\mu_k = 0.3$, the static coefficient of friction $\mu_s = 0.35$, and the coefficient of restitution $e = 0.4$ are used. These values are constant through the investigation. The analysis is performed for different values of the clearance c, varying the nominal angular velocity of link 1, ω_{10}. The torque of the motor acting at joint A is chosen as $M_m = M_0(1 - \omega_1/\omega_{10})$, where $M_0 = 1$ N m.

Fig. 4(a) shows the vertical trajectory for the center of mass G_2 of link 2, y_{G_2}, in the state space for zero clearance ($c = 0$ mm). On the three-dimensional graphic, the co-ordinate of the position $y_{G_2}(t)$ is plotted along the co-ordinate $y_{G_2}(t + T)$ and the co-ordinate $y_{G_2}(t + 2T)$, where T is the time lag. The trajectory is a closed loop and the motion is periodic. In this case, the largest Lyapunov exponent is zero ($\lambda_l = 0$) and all the other exponents are less than zero, that is, a periodic orbit.

Fig. 4(b) shows the vertical trajectory y_{G_2} in the state space for non-zero clearance $c = 1$ mm, and $\omega_{10} = 200$ r.p.m. The curve is not closed, that is, an unstable orbit. The largest Lyapunov exponent is positive ($\lambda_l = 31.24$), denoting the chaotic behavior of the system.

Next, the largest Lyapunov exponent is computed for a set of simulation results for different values of the angular velocity ω_{10}. Fig. 5 shows the results for the clearances: $c = 0.5$ mm (Fig. 5(a)), $c = 1$ mm (Fig. 5(b)), and $c = 1.5$ mm (Fig. 5(c)). For constant clearance ($c = constant$) and for larger values of the angular velocity ω_{10} one can obtain larger values of the

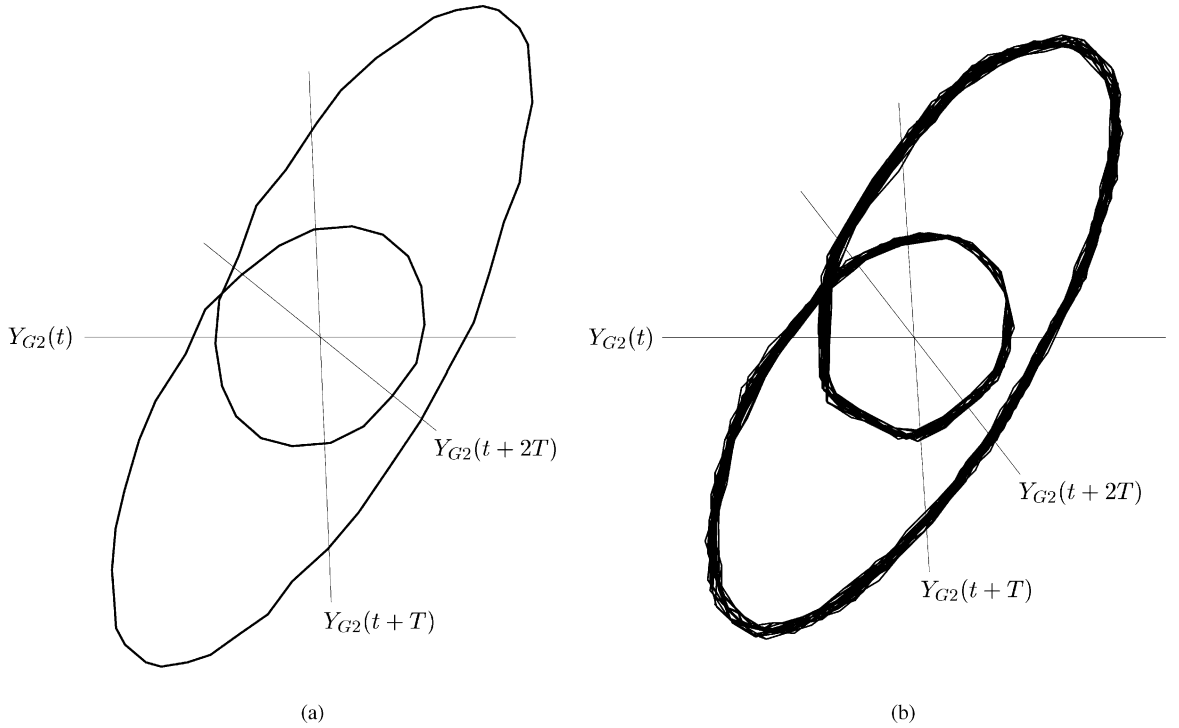

Fig. 4. Trajectory of the vertical co-ordinate y_{G_2} in the state space for (a) zero clearance ($c = 0$ mm), (b) non-zero clearance ($c = 1$ mm).

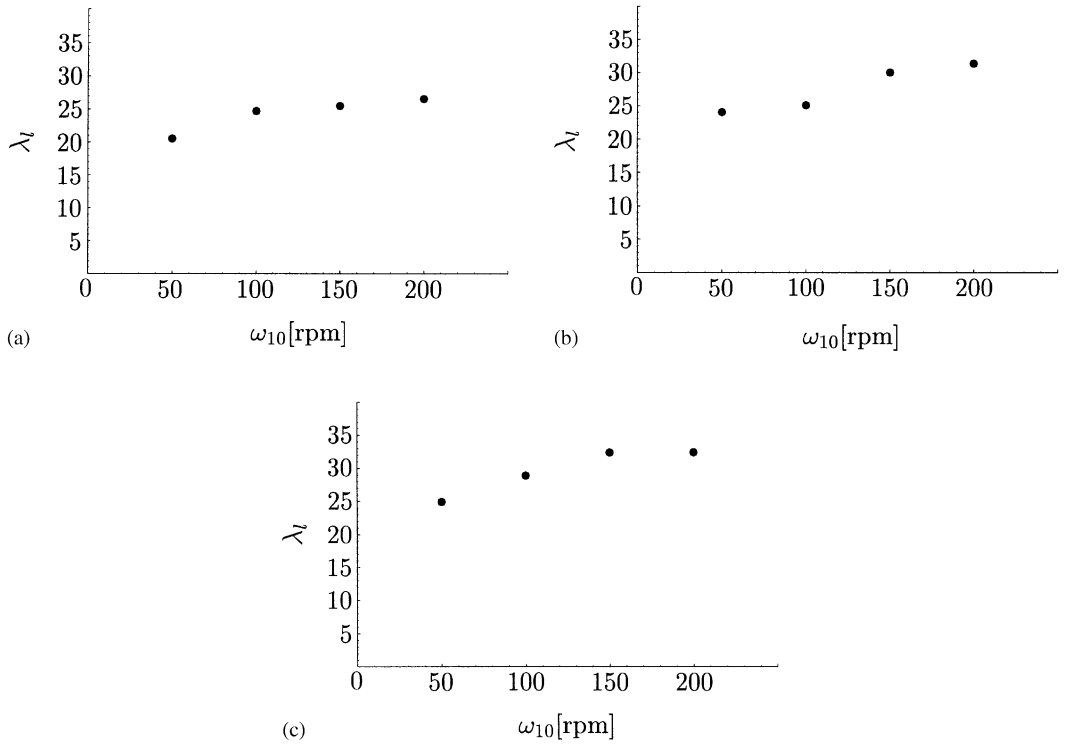

Fig. 5. Largest Lyapunov exponent computed for a set of values of the nominal angular velocity ω_{10} and for the various clearances: (a) $c = 0.5$ mm, (b) $c = 1$ mm, (c) $c = 1.5$ mm.

Lyapunov exponent λ_l. For $c = 0.5$ mm, $\omega_{10} = 50$ r.p.m, it results $\lambda_l = 20.54$, and for $c = 0.5$ mm, $\omega_{10} = 200$ r.p.m, it results $\lambda_l = 26.55$. Also, for constant angular velocity ($\omega_{10} = constant$) and larger values of the clearance c one can obtain larger values of the Lyapunov exponent λ_l. For $\omega_{10} = 100$ r.p.m, $c = 0.5$ mm, it results $\lambda_l = 24.66$, and for $\omega_{10} = 100$ r.p.m, $c = 1.5$ mm, it results in $\lambda_l = 28.90$.

Appendix A. Nomenclature

L_i	length of link i ($i = 1, 2, 3$)
l_i	width of link i
c	length of the clearance between links 2 and 3
m_i	mass of link i
$\mathbf{r}_{G_i}$	position of the center of mass G_i for link i
$\mathbf{v}_{G_i}$	linear velocity vector of the center of mass G_i for link i
$\mathbf{a}_{G_i}$	linear acceleration vector of the center of mass G_i for link i
I_{G_i}	mass moment of inertia for link i about an axis perpendicular to the plane of mechanism, through the center of mass of the link

θ_i angle between link i and the horizontal axis Ox
ω_i angular velocity of link i
α_i angular acceleration of link i
T_i kinetic energy for link i
μ_k coefficient of kinetic friction
μ_s coefficient of static friction
e coefficient of restitution
g gravitational acceleration
$\mathbf{G}_i$ gravitational force acting on link i
M_m torque of the motor acting on link 1

References

[1] F. Farahanchi, S.W. Shaw, Chaotic and periodic dynamics of a slider-crank mechanism with slider clearance, Journal of Sound and Vibration 177 (3) (1994) 307–324.
[2] H.D.I. Abarbanel, Tools for Analysing Observed Chaotic Data, Springer, New York, 1995.
[3] H.D.I. Abarbanel, Analysis of Observed Chaotic Data, Springer, New York, 1996.
[4] H.D.I. Abarbanel, T.W. Frison, L.S. Tsimring, Time-domain analysis of non-linear and chaotic signals, IEEE Signal Processing Machine (May 1998) 49–65.
[5] A.H. Nayfeh, B. Balachandran, Applied Non-linear Dynamics, Wiley, New York, 1995.
[6] J.F. Deck, S. Dubowski, On the limitations of predictions of the dynamic response of machines with clearance connections, Flexible Mechanisms, Dynamics, and Analysis 47 (1992) 461–469.
[7] B.J. Gilmore, R.J. Cipra, Simulation of planar dynamic mechanical systems with changing topologies: Part I—characterization and prediction of the kinematic constraint changes, Part II—implementation strategy and simulation results for example dynamic systems, American Society of Mechanical Engineers, Journal of Mechanical Design 113 (1991) 70–83.
[8] C. Conti, P. Corron, P. Michotte, A computer aided kinematic analysis system for mechanism design and computer simulation, Mechanism and Machine Theory 27 (1992) 563–574.
[9] F. Pfeiffer, Complimentarity problems of stick-slip vibrations, American Society of Mechanical Engineers Dynamics and Vibration of Time-Varying Systems and Structures 56 (1993) 43–50.
[10] R.M. Brach, Rigid body collisions, American Society of Mechanical Engineers, Journal of Applied Mechanics 56 (1989) 133–138.
[11] M. Jean, J.J. Moreau, Unilaterality and dry friction in the dynamics of rigid body collections, Proceedings of the Contact Mechanics International Symposium, Lausanne, 1992, pp. 31–48.
[12] D.B. Marghitu, Y. Hurmuzlu, Three dimensional rigid body impact with multiple contact points, American Society of Mechanical Engineers, Journal of Applied Mechanics 62 (1995) 725–732.
[13] D.B. Marghitu, Impact of flexible link with solid lubrication, Journal of Sound and Vibration 205 (4) (1997) 712–720.